SUPPLEMENTARY INFORMATION

Designing Bifunctional Catalysts for the One-pot Conversion of CO_2 to Sustainable Marine Transportation Fuels

Maciej G. Walerowski[a], Matthew E. Potter[b, c, d], Elizabeth Burke[a], Stylianos Kyrimis[e], Lindsay-Marie Armstrong[e] and Robert Raja[a*]

[a] School of Chemistry, University of Southampton, Southampton, SO17 1BJ, UK.

[b] Chemistry Department, University College London, London, WC1E 6BT, UK.

[c] UK Catalysis Hub, Harwell Research Complex, Harwell, OX11 0FA, UK.

[d] Department of Chemistry, University of Bath, Bath, BA2 7AY, UK.

[e] School of Engineering, University of Southampton, Southampton, SO17 1BJ, UK.

*R.Raja@soton.ac.uk

Contents

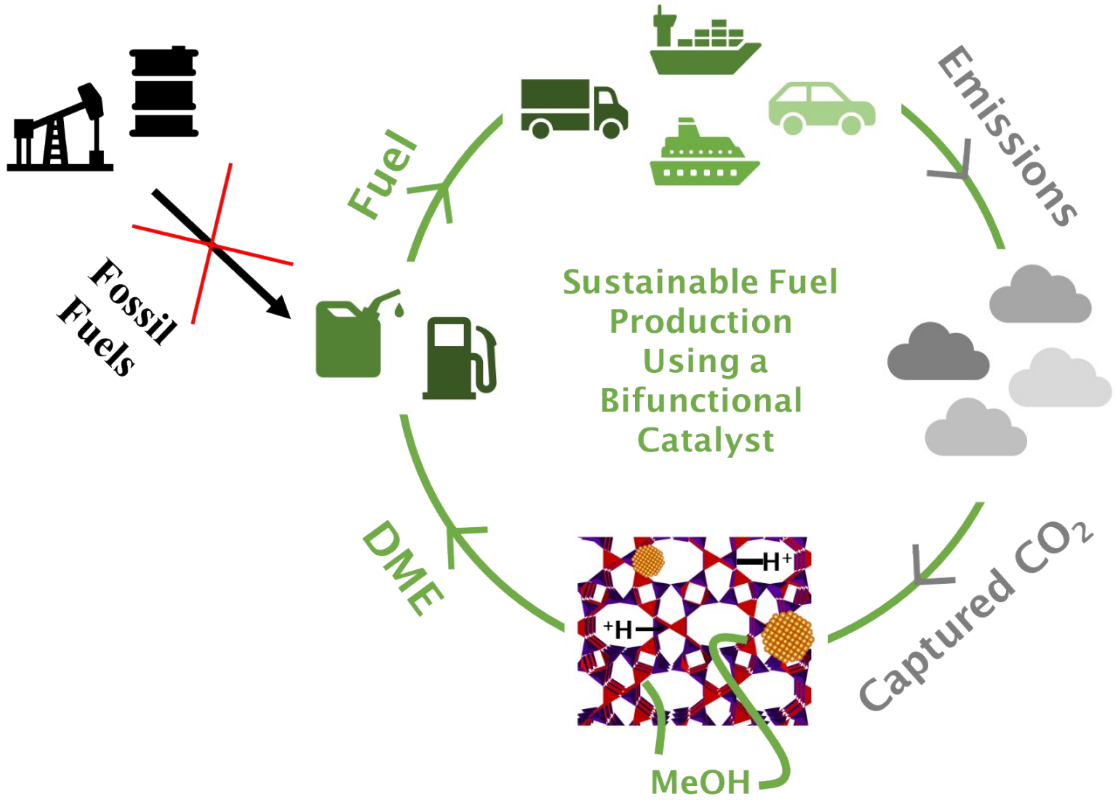

Fig. S1 Using bifunctional catalysts to produce the sustainable fuel dimethyl ether via a circular carbon economy.

1 Synthetic procedures

1.1 Solid acids

1.1.1 SAPO-11

A large batch of SAPO-11 was synthesised as follows, as per published approaches.[1] Deionised water (70 mL, GPR Rectapur, 0.8 µs/cm) was added to a 1 L Teflon beaker. Aluminium isopropoxide (58.35 g, >98%, Sigma-Aldrich) was slowly added to the beaker and stirred for 15 minutes. In a separate glass beaker, deionised water (56 mL, GPR Rectapur, 0.8 µs/cm) and phosphoric acid (32.29 g, >85 wt% in H_2O, Sigma-Aldrich) were mixed. The aqueous phosphoric acid solution was then slowly added to the aluminium solution and stirred for 1 hour. Dipropylamine (28.33 g, 99%, Sigma-Aldrich) was then slowly added dropwise to the Teflon beaker and stirred for further 2 hours. Ludox AS-40 (8.42 g, 40 wt% suspension in water, Sigma-Aldrich) then added dropwise to the Teflon beaker and mixed for further 3 hours. The uniform white gel of ratio 1:0Al:1.0P:0.2Si:1.0DPA:25H_2O was then crystallised in a Teflon lined Parr batch reactor at 200°C for 48 hours with no mixing. Once crystallisation was complete, the Parr reactor was immediately quenched in ice and the white solid separated via centrifugation. The white solid was then washed twice with water and any unreacted/amorphous material was separated via sedimentation and skimming. Crystalline material was dried overnight at 70°C and then calcined at 600°C for 40 hours in flowing air with a 2.5°C/min ramp rate to yield a fine, white crystalline material.

1.1.2 SAPO-34

A large batch of SAPO-34 was synthesised as follows, as per published approaches.[2] TEAOH (91.06 g, 35 wt% in H_2O, Sigma-Aldrich) was added to a 1 L Teflon beaker. Aluminium isopropoxide (45.16 g, ≥98%, Sigma-Aldrich) was then slowly added to the TEAOH solution and mixed for 1 hour. Silica fumed (1.99 g, Sigma-Aldrich) was then slowly added to the beaker and mixed for a further 1 hour. Deionised water (35.94 g, 0.8 µS/cm, VWR Water GPR Rectapur) and phosphoric acid (25.27, ≥85wt% in H_2O, Sigma-Aldrich) were gently mixed in a separate glass beaker and then added dropwise into the Teflon beaker and mixed for a further 2 hours. The uniform white gel of ratio 1.0Al:1.0P:0.15Si:1.0TEAOH:9H_20 was then crystallised in a Teflon lined Parr batch reactor at 200°C for 72 hours with no mixing. Once crystallisation was complete, the Parr reactor was immediately quenched in ice. White solid was then separated via centrifugation and washed twice with DI water. The white solid was then dried overnight in a 70°C oven to yield a fine, white crystalline material. The material was then calcined at 600°C for 16 hours in flowing air with a 2.5°C/min ramp rate to yield a white crystalline material.

1.2 CuZnO/SAPO-11 and CuZnO/SAPO-34 bifunctional catalysts

All the CuZnO/SAPO-X catalysts had a target 2:1:10 Cu:Zn:SAPO mass ratio and all were calcined at 300°C for 5 hours in flowing air with a 2.5°C/min ramp rate followed by reduction at 300°C for 4 hours in 300 mL/min H_2 in N_2 flow with a 2.5°C/min ramp rate.

1.2.1 Impregnation and drying (ID)

Deionised water (18.2 MΩ), copper (II) acetate monohydrate (98+% extra pure, Acros Organics) & zinc acetate dihydrate (98% extra pure, Acros Organics) were added to a RBF situated in a 70°C oil bath and mixed for 15 minutes. Calcined SAPO-X was then added to the dark blue clear solution and mixed for further 30 minutes. The mixture was then evaporated to dryness and the resulting pale green powder was then calcined to yield a fine brown material and reduced to yield a dark brown/pale black material.

1.2.2 Oxalate gel deposition precipitation (OG)

The OG methodology is an adapted co-precipitation methodology used by Sun *et al.* for the synthesis of ultrafine particle Cu/ZnO/Al_2O_3 catalysts.[3] Copper (II) nitrate trihydrate (EMSURE, Supelco/Sigma-Aldrich) and zinc nitrate hexahydrate (99% metal basis, Alfa Aesar) were dissolved in ethanol (15 mL, 99.8%, Fisher) to yield a clear, blue solution. Calcined SAPO-X was added to the metal solution and stirred vigorously for 1 hour. Oxalic acid (puriss. p.a. anhydrous ≥ 99.0%, Sigma-Aldrich) was then added to the metal/SAPO-X mixture and the dark blue cloudy mixture turned pale blue and gel-like. The gel was stirred for a further 1 hour. The solid was then separated via centrifugation, thoroughly washed with water and dried overnight in a 70°C oven. The blue/white solid was ground to improve homogeneity, calcined to yield a uniform brown powder and then reduced to yield a fine grey powder.

1.2.3 Deposition precipitation (DP)

The DP method is an adapted co-precipitation method used by Baltes *et al.* for the synthesis of Cu/ZnO/Al_2O_3.[4] Deionised water and calcined SAPO-X were added to a round bottom flask situated in a 70°C oil bath. Solutions of 0.6 mol/L $Cu(NO_3)_2$ and 0.3 mol/L $Zn(NO_3)_2$ were pumped into the RBF and pH was maintained between 5.25 and 5.50 using a 1 mol/L Na_2CO_3 solution. Once the metal solution addition was complete, the mixture was free aged for 1 hour at 70°C under stirring with no further pH adjustments. The blue solid was then filtered under vacuum and thoroughly washed with deionised water, dried overnight in a 70°C oven, calcined to yield a grey-brown powder and reduced to yield a brown/black powder.

1.2.4 Physical mixture (PM)

Calcined and reduced 2:10 Cu/SAPO-X ID and 1:10 ZnO/SAPO-X ID powders were thoroughly mixed in a 1:1 ratio before pelletisation to ensure a close contact between the two catalysts.

1.2.5 $Cu/ZnO/Al_2O_3$ (CZA)

An optimised 10:5:1 $Cu/ZnO/Al_2O_3$ catalyst was produced via co-precipitation as described by Baltes *et al.*[4] Deionised water was added to a round bottom flask situated in a 70°C oil bath. Solutions of 0.6 mol/L $Cu(NO_3)_2$, 0.3 mol/L $Zn(NO_3)_2$ and 0.1 mol/L $Al(NO_3)_3$ were pumped into the RBF and pH was maintained between 6.75 and 7.00 using a 1 mol/L Na_2CO_3 solution. Once the metal solution addition was complete, the mixture was free aged for 1 hour at 70°C under stirring with no further pH adjustments. The bright blue solid was then filtered under vacuum and thoroughly washed with deionised water, dried overnight in a 70°C oven, calcined to yield a brown powder and reduced to yield a black powder.

2 Reactor setup

Catalysis was performed in a custom built reactor which comprised of hydrogen, argon and carbon dioxide cylinders, three mass flow controllers, laptop computer to control the mass flow controllers and mass spectrometer, heating jacket for the reactor, emergency proportional pressure relief valve, pressure gauge, backpressure regulator, hotplate to heat the backpressure regulator and a mass spectrometer.

Catalyst powder (~0.4 g) was pelletised at 4 tonnes using a Graseby Specac pellet press for 10 seconds to yield self-supporting discs of 2.5 cm diameter. The discs were then crushed and sieved 5 times between 300 and 500 µm sieves to yield catalyst particles in the 300-500 µm range. The catalyst particles (0.300 g) were then sandwiched between 5 and 17 cm layers of 1 mm borosilicate beads and the reactor placed inside the heating jacket.

For the dual bed, the reactor was packed in a different manner. The reactor outlet was plugged with glass wool as before, a 5 cm layer of 1 mm borosilicate beads was then placed on top, the pelletised SAPO-X (300-500 µm) particles (0.230 g) were then added on top, followed by a second 3 cm layer of borosilicate beads, followed by the pelletised $Cu/ZnO/Al_2O_3$ (300-500 µm) particles (0.070 g) and then by a third and final layer of borosilicate beads all the way to the top of the reactor. For the granule mixing, the pelletised SAPO-X (300-500 µm, 0.230 g) and pelletised $Cu/ZnO/Al_2O_3$ (300-500 µm, 0.070 g) particles were mixed to give a single bed. For the powder mix, SAPO-X powder (0.230 g) and $Cu/ZnO/Al_2O_3$ powder (0.070 g) was physically mixed and pelletised and then loaded to give a single catalyst bed. In terms of separation therefore: dual bed > granule mixing > powder mixing with dual bed having the greatest spatial separation.

The catalyst was then reduced in a 60 mL/min H_2 flow at 300°C for 2 hours before temperature was reduced to 260°C. Reaction gas mixture of 5.5 Ar, 15 CO_2 and 45 H_2 mL/min was flown into the reactor and pressure was built up to 40 bars. As soon as the reaction pressure was attained, mass spectrometric analysis was begun. The reaction was allowed to proceed for a minimum of an hour after which steady state was obtained. Mass spectrometric measurements were taken every ~10 seconds and the results presented are an average over a period of 15 minutes which is approximately equal to 100 analysis points.

Temperature, gas flow rate and mass spectrometric calibrations were performed previously to ensure accurate results and quantification.

Equations S1-S4 were used to calculate CO_2 conversion and product selectivity as these approaches are most commonly used in literature.[5–9] Equation S5 was used to calculated carbon mass balance by comparing the inlet and outlet moles of carbon.

Argon was used as an internal standard.

$$CO_2\ Conversion = \frac{CO_{2\ in} - CO_{2\ out}}{CO_{2\ in}}\ x\ 100$$

Equation S1

$$CO\ Selectivity = \frac{n_{CO}}{\sum n_{(CO + MeOH + 2DME)}}\ x\ 100$$

Equation S2

$$MeOH\ Selectivity = \frac{n_{MeOH}}{\sum n_{(CO + MeOH + 2DME)}}\ x\ 100$$

Equation S3

$$DME\ Selectivity = \frac{2n_{DME}}{\sum n_{(CO + MeOH + 2DME)}} x\ 100$$

Equation S4

$$Carbon\ Mass\ Balance = \frac{\sum n_{(CO_{2\ out} + CO + MeOH + 2DME)}}{nCO_{2\ in}}$$

Equation S5

$$Water\ Space\ Time\ Yield = \frac{n_{Water}\ x\ M_{Water}}{m_{cat}} x\ 60$$

Equation S6

Where the $CO_{2\ in}$ and $CO_{2\ out}$ are the inlet and outlet molar flow rates (mol/min) of CO_2 respectively, *n* (mol/min) is the outlet molar flow rate of the species of interest, *M* is the molar mass of the species of interest and m_{cat} is the mass of catalyst used.

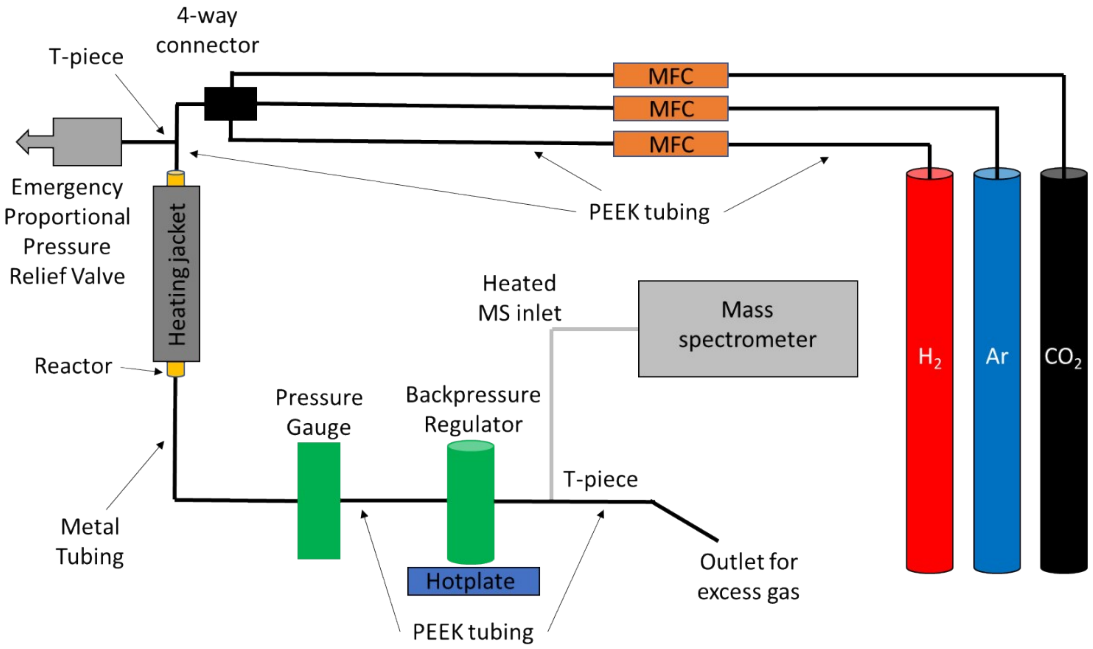

Fig. S2 Schematic of continuous flow high-pressure fixed bed reactor system used for testing of CO_2 to DME bifunctional catalysts.

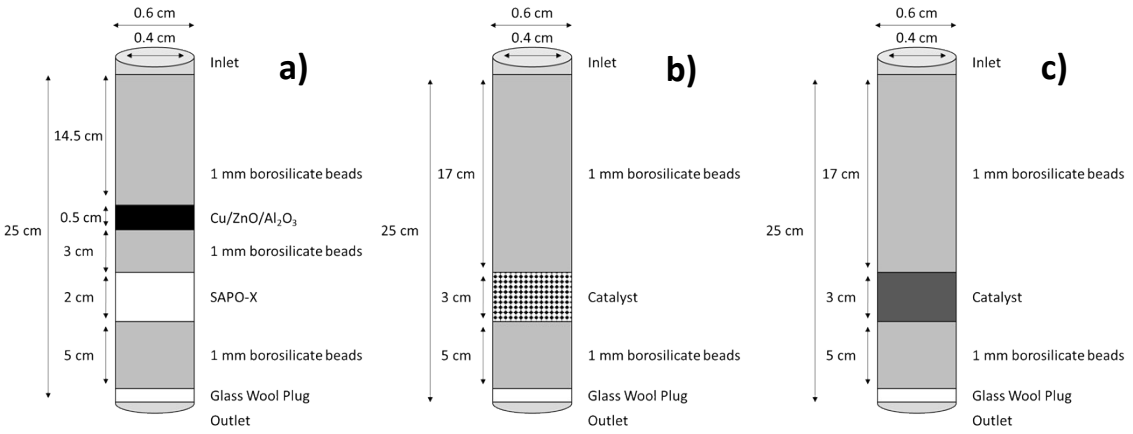

Fig. S3 Different reactor set-ups used for testing of bifunctional catalysts: **a)** Dual bed (DB) **b)** granule mixing (GM) and **c)** powder mixing (PM).

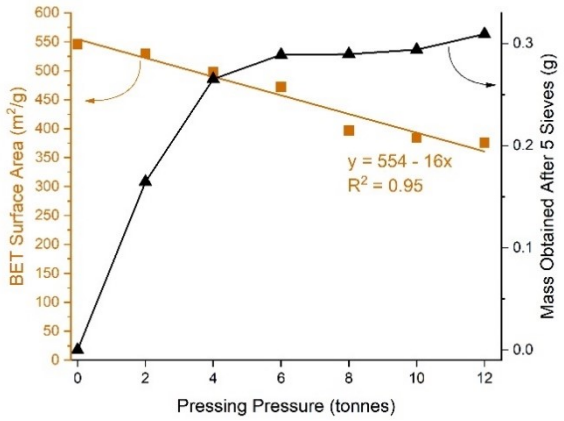

Fig. S4 Impact of pressing pressure on the surface area of SAPO-34 and the mass gained of desired size fraction.

3 Catalyst characterisation

3.1 Elemental analysis

ICP-MS analysis was performed at the National Oceanographic Centre Southampton. Samples (~10 mg) were fully digested in a hot mixture of concentrated H_2SO_4 (1 mL), HNO_3 (1 mL) and HF (0.75 mL) overnight. Digested solutions were subsequently diluted in water and diluted further using dilute HNO_3. The samples were analysed on a ThermoFisher XSeries2 ICP-MS operating in standard and CCT mode at the School of Ocean and Earth Science at the University of Southampton. Calibration was carried out using synthetic standards prepared from Inorganic Venture single element ICP-MS standards. The samples and standards both contained In and Re and 5ppb to act as internal standards.

3.2 Carbon Hydrogen Nitrogen Analysis (CHN)

CHN analysis was performed by the elemental analysis service team at London Metropolitan University. Samples (~5 mg) were weighed using a high precision Mettler Toledo scale and analysed using a ThermoFlash 2000 in duplicate.

Table S1 Coke content of fresh and spent CuZnO/SAPO-X (where X = 11 or 34) catalysts prepared via the ID, OG or DP methods which were used for time-on-stream stability studies.

Synthesis Method	Fresh catalyst carbon content (%)		Spent catalyst carbon content (%)		Carbon gained (wt%)	
	-11	-34	-11	-34	11	34
ID	0.25	0.25	0.52	0.34	0.27	0.09
OG	0.35	0.18	0.31	0.21	-0.04	0.03
DP	0.23	0.12	0.37	0.22	0.14	0.10

3.3 Powder X-ray diffraction (PXRD)

PXRD characterisation was performed using a Bruker D2 Phaser instrument. Patterns were obtained using Cu Kα radiation (λ = 1.54184 Å) at 30 kV voltage and 10 mA current using a 0.6 mm slit. Patterns were obtained in the 5-60° 2θ range with 0.02° increments and 0.2 s per step.

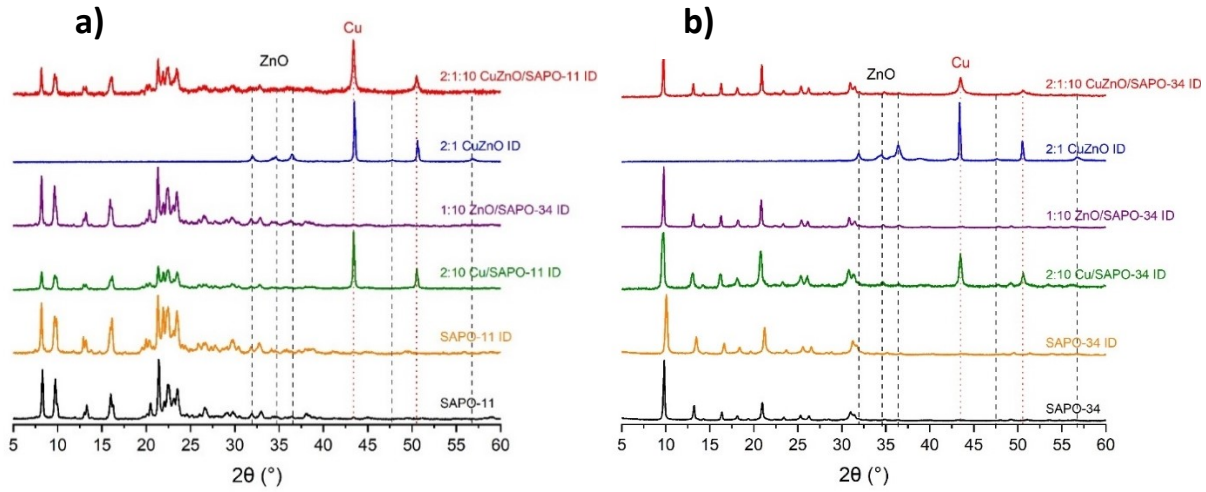

Fig. S5 PXRD patterns of various **a)** M/SAPO-11 and **b)** M/SAPO-34 catalysts prepared via the ID method showing the emergence of peaks attributed to Cu and ZnO.

3.4 Surface area and porosity

Surface area and porosity characterisation was performed using Micromeritics Tristar II 3020 analyser. N_2 was used as the adsorptive, and a liquid N_2 bath was utilised. Analysis performed between 0.00 and 0.95 p/p_0 (relative pressure). 124 adsorption and 30 desorption points were used to obtain the full physisorption isotherm. BET surface area and pore volume calculated automatically by the Micromeritics Tristar II 3020 software. Samples (~0.15 g) were thoroughly degassed for a minimum of 21 hours using a Micrometrics Vac Prep 062 system by heating them under vacuum at 120°C, with final pressure of ~100 mTorr.

Synthesis Method	Total Surface Area (m^2/g)		Micropore Surface Area (m^2/g)		Total Pore Volume (cm^3/g)		Micropore Pore Volume (cm^3/g)	
	-11	-34	-11	-34	-11	-34	-11	-34
Undoped	135	546	109	512	0.08	0.30	0.05	0.26
ID	21	330	8	308	0.05	0.19	0.002	0.15
OG	92	245	62	218	0.12	0.17	0.03	0.11
DP	30	274	20	261	0.03	0.16	0.01	0.13

Table S2 Surface area and pore volumes of CuZnO/SAPO-X (where X = 11 or 34) catalysts prepared via different synthetic methods.

Table S3 Surface area and pore volume of M/SAPO-X (where X = 11 or 34) catalysts prepared via the ID method.

Synthesis Method	Total Surface Area (m^2/g)		Micropore Surface Area (m^2/g)		Total Pore Volume (cm^3/g)		Micropore Pore Volume (cm^3/g)	
	-11	-34	-11	-34	-11	-34	-11	-34
SAPO-X ID	60	511	44	484	0.06	0.29	0.02	0.25
2:10 Cu/SAPO-X ID	21	402	12	363	0.03	0.23	0.005	0.18
1:10 Zn/SAPO-X ID	12	370	3	344	0.02	0.20	0.000	0.17
2:1 CuZnO ID	13		5		0.05		0.001	

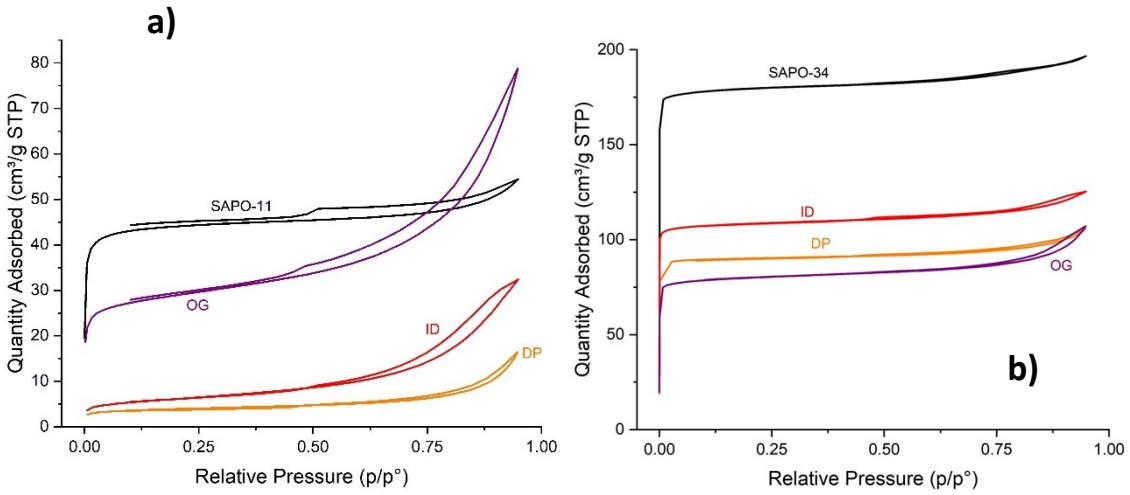

Fig. S6 Nitrogen physisorption isotherms of **a)** CuZnO/SAPO-11 and **b)** CuZnO/SAPO-34 bifunctional catalysts prepared via different synthesis methodologies.

3.5 Scanning electron microscopy (SEM)

Scanning electron microscopy (SEM) characterisation was performed using a JEOL JSM-7200F field emission scanning electron microscope. 10 kV acceleration voltage was used with 93 µA emission current. An Oxford Instrument backscattered electron detector (BED-C) was used for imaging. Working distance ranged between 6 and 12 mm. Sample was imaged directly on tape without prior sputter coating.

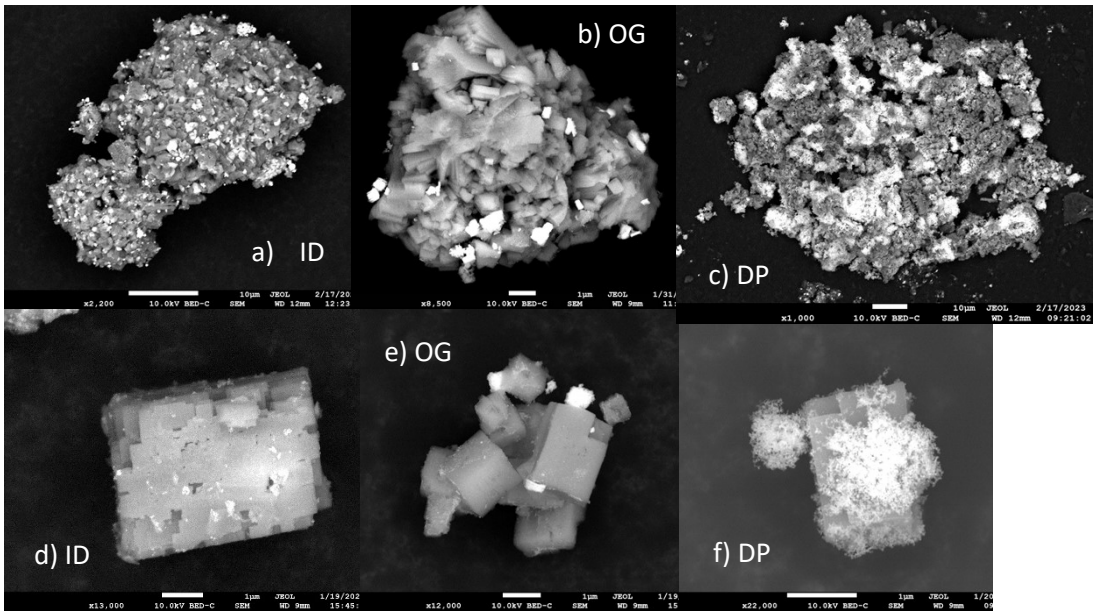

Fig. S7 SEM images of CuZnO/SAPO-X (where X = 11 (top) or 34 (bottom)) catalysts prepared via different methods showing the interaction of metallic species (bright spots) with SAPO crystals.

3.6 Transmission electron microscopy (TEM)

TEM imaging was performed using a FEI Tecnai T12 instrument at an acceleration voltage of 120 kV. The instrument was equipped with a Morada G3 (16 MP) detector for digital imaging. The sample powder was suspended in ethanol and loaded directly onto carbon and formvar coated copper TEM grids. The characterisation was performed at the Biological Imaging Unit at the University Hospital Southampton.

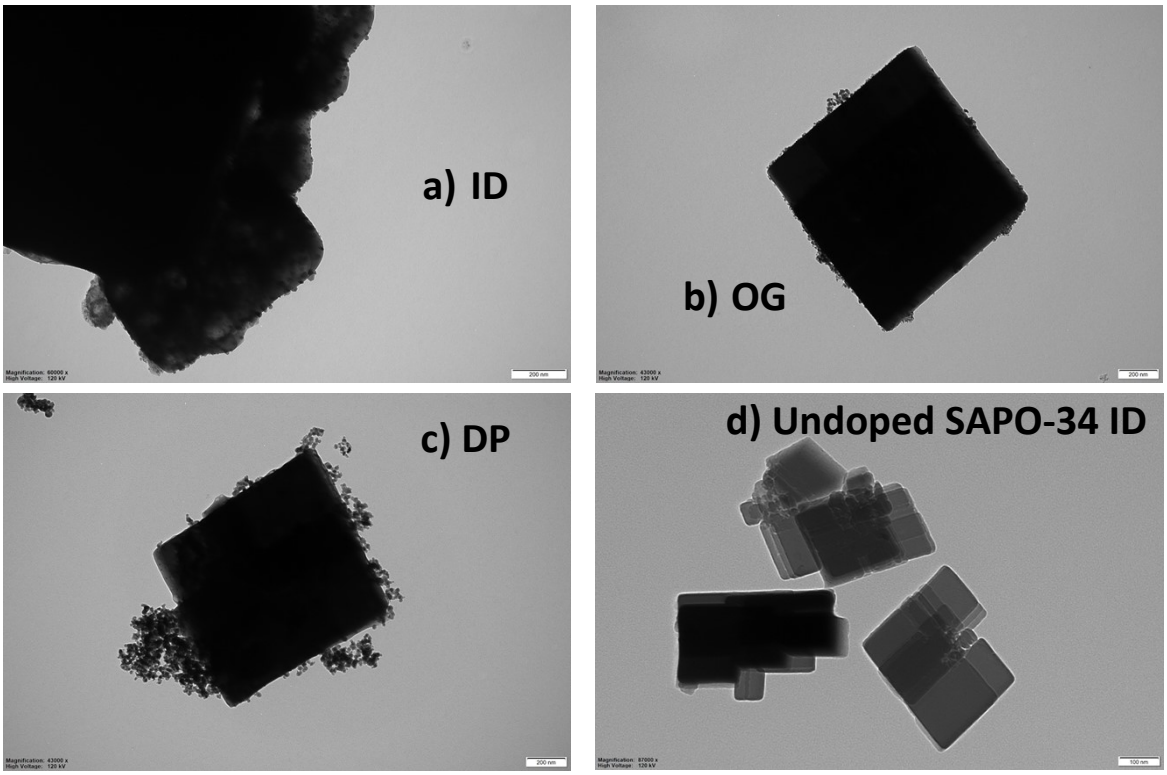

Fig. S8 TEM images of fresh CuZnO/SAPO-34 catalysts prepared via different methods showing the interaction between CuZnO nanoparticles and cubic SAPO-34 crystals. Undoped SAPO-34 which has undergone the ID methodology has been included for reference to verify lack of nanoparticles.

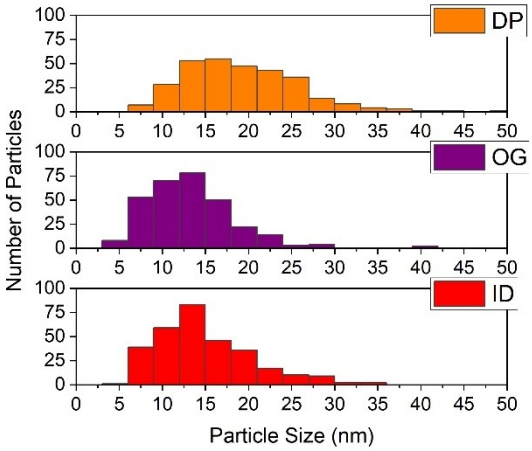

Fig. S9 Particle size histograms of fresh CuZnO/SAPO-34 catalysts prepared via different methods. Results are based on a measurement of 300 particles.

3.7 NH_3 temperature programmed desorption (TPD) acid site characterisation

NH_3-TPD experiments were performed on Quantachrome ChemBET Pulsar TPR/TPD instrument. 0.2 g of 100 – 425 µm pelletised sample was dried at 550˚C for 2 hours under a 24 mL/min He and 6 mL/min O_2 flow. Sample was then cooled down to 150˚C and put under a 30 mL/min flow of 5% NH_3/He, the sample was held at 150˚C for 2 hours. Flow was then changed to 30 mL/min He and sample held at 150˚C for further 2 hours. System was then heated to 600˚C at a rate of 5˚C/min and evolution of NH_3 as a function of temperature was monitored. The system was then held at 600˚C for 1 hour to fully desorb any remaining NH_3.

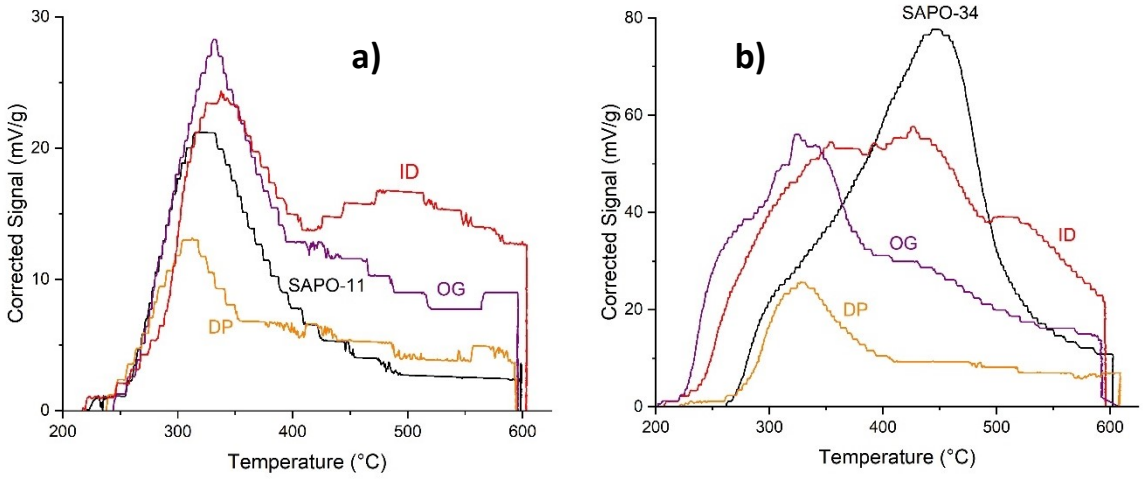

Fig. S10 NH_3-TPD profiles of **a)** CuZnO/SAPO-11 and **b)** CuZnO/SAPO-34 catalysts prepared via the ID, OG and DP methods.

Table S4 Total integrated area of NH_3-TPD peaks of CuZnO/SAPO-X (where X = 11 or 34) catalysts prepared via the ID, OG and DP methods.

Synthesis Method	Total Integrated Area (mV*s/g)	
	-11	-34
Undoped	24 088	90 616
ID	47 706	110 850
OG	39 418	89 183
DP	18 682	33 975

3.8 X-ray absorption fine structure (XAFS)

The XAFS spectra for the Cu and Zn K-edges (8.979 and 9.659 keV respectively) were collected at the general purpose XAS beamline, B18 at the Diamond Light Source (UK) and accessed through the UK Catalysis Hub, block allocation group (BAG, SP-29721-6). The collimated, white X-ray beam is incident on a Si(111) double crystal monochromator and a Pt-coated focusing mirrors, covering the energy range 6.34 keV to 9.98 keV. The beam size at the sample was approximately 1.0 x 1.0 mm^2 (V x H) and the photon flux was ~1011 ph/s (no attenuation). The XAFS spectra were collected in transmission mode and the intensity of the incident beam (I_0) and the transmitted beam (I_t) was monitored by ionization chambers (filled with a mixture of He, N_2, and Ar). Samples were diluted with cellulose before pressing into 13mm diameter pellets. The XAFS spectra of each sample were measured at least 3 times in transmission mode at room temperature and merged to improve the signal-to-noise ratio. Zn and Cu metal foil was measured simultaneously for each sample as a reference for energy calibration. XAFS data (kmax = 16) was analyzed using the Demeter software package which includes Athena and Artemis. [10]

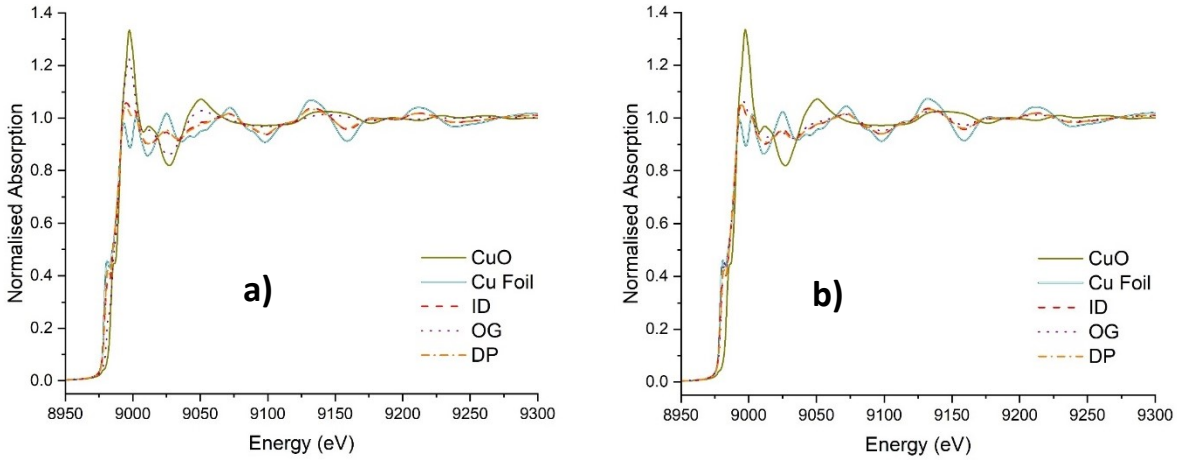

Fig. S11 Cu K Edge XAFS spectra of **a)** CuZnO/SAPO-11 and **b**) CuZnO/SAPO-34 catalysts prepared via the ID, OG and DP methods. Spectra of Cu(0) and CuO standards included for reference.

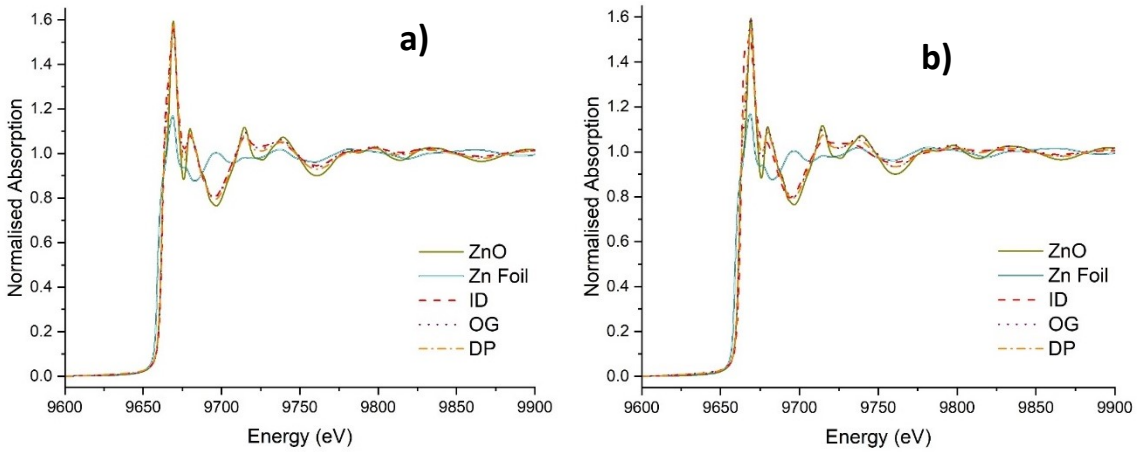

Fig. S12 Zn K Edge XAFS spectra of **a)** CuZnO/SAPO-11 and **b)** CuZnO/SAPO-34 catalysts prepared via the ID, OG and DP methods. Spectra of Zn(0) and ZnO standards included for reference.

Table S5 Average oxidation states of CuZnO/SAPO-X (where X = 11 or 34) catalysts prepared via the ID, OG and DP methods.

Synthesis Method	Average Cu oxidation state		R Factor for Cu LCF		Average Zn oxidation state		R Factor for Zn LCF	
	-11	-34	-11	-34	-11	-34	-11	-34
ID	0.50	0.35	0.001	0.001	2	2	0.016	0.041
OG	1.43	0.41	0.001	0.003	2	2	0.009	0.005
DP	0.36	0.35	0.001	0.002	2	2	0.004	0.011

Oxidation state was determined using a linear combination fitting (LCF) of Cu(0), Zn(0), CuO and ZnO standards.

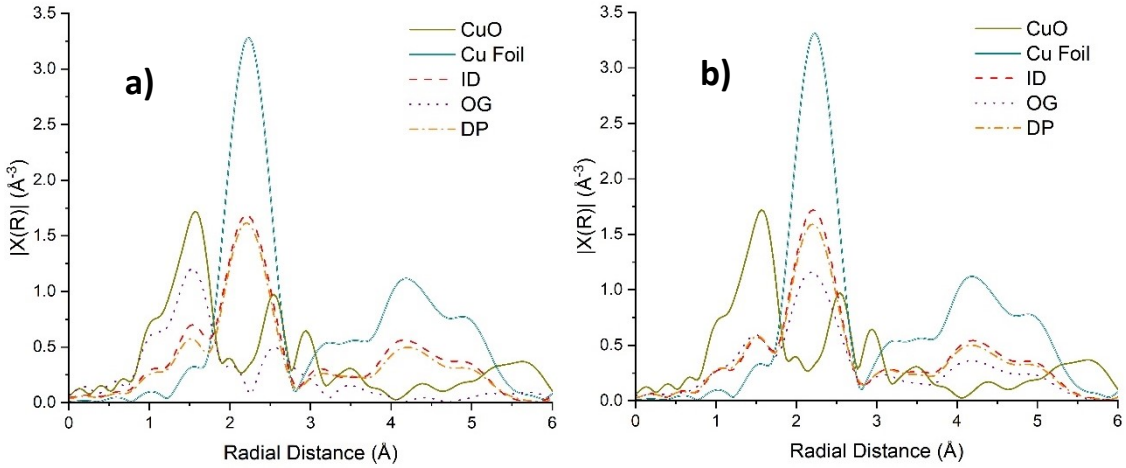

Fig. S13 Fourier transform of the k2-weighted X Cu K Edge EXAFS data of **a)** CuZnO/SAPO-11 and **b)** CuZnO/SAPO-34 catalysts prepared via the ID, OG and DP methods. Cu(0) and CuO standards included for reference.

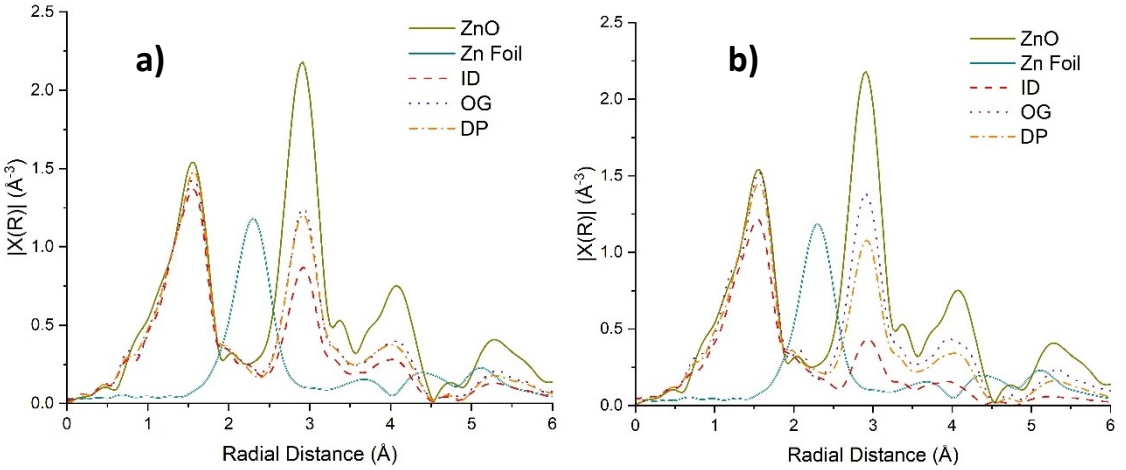

Fig. S14 Fourier transform of the k2-weighted X Zn K Edge EXAFS data of **a**) CuZnO/SAPO-11 and **b)** CuZnO/SAPO-34 catalysts prepared via the ID, OG and DP methods. Zn(0) and ZnO standards included for reference.

Table S6 EXAFS Fitting for Zn K-edge data of CuZnO/SAPO-X (where X = 11 or 34) catalysts prepared via the ID, OG and DP synthetic methods.

Synthesis Method	Scattering Path	Coordination number		$2\sigma^2$ (Å^2)		*R* (Å)		E_f (eV)		*R* factor	
		-11	-34	-11	-34	-11	-34	-11	-34	-11	-34
ID	Zn-O	4.9(1)	5.13(7)	0.0051(3)	0.0067(2)	1.964(4)	1.965(3)	3.0(5)	1.4(3)	0.006	0.003
	Zn-Zn	19(1)	10.5(5)	0.0177(6)	0.0185(5)	3.246(6)	3.244(5)				
OG	Zn-O	5.4(2)	4.9(2)	0.0060(6)	0.0046(6)	1.964(8)	1.967(8)	3.5(7)	4.5(9)	0.010	0.018
	Zn-Zn	18(1)	29(2)	0.0137(6)	0.0170(7)	3.235(8)	3.246(9)				
DP	Zn-O	4.7(2)	4.9(1)	0.0045(5)	0.0049(4)	1.965(6)	1.962(5)	4.5(7)	3.9(6)	0.010	0.006
	Zn-Zn	25(1)	21(1)	0.0169(6)	0.0163(5)	3.246(7)	3.246(6)				

Amplitude reduction factor of 0.693 was determined from fitting of Zn(0) using two Zn-Zn paths with bond lengths of 2.665 and 2.913 Å each with a coordination number of 6. Fitting of the second shell Zn-Zn pathway was required to ensure a satisfactory fit, however the high $2\sigma^2$ and coordination values indicate that there is some uncertainty in the second shell and so these results are not discussed further.

3.9 Wavelet transformation (WT)

MorletE programme was used for WT which employs the Morlet mother function.[11,12] WT was performed on K edge, $k^2X(k)$ input data which was previously utilised for EXAFS analysis. WT of Cu K edge data employed η of 5, σ of 2, 0-11 k range and 0.1-6 R range. WT of Zn K edge data employed η of 5, σ of 2, 0-14 k range and 0.1-6 R range.

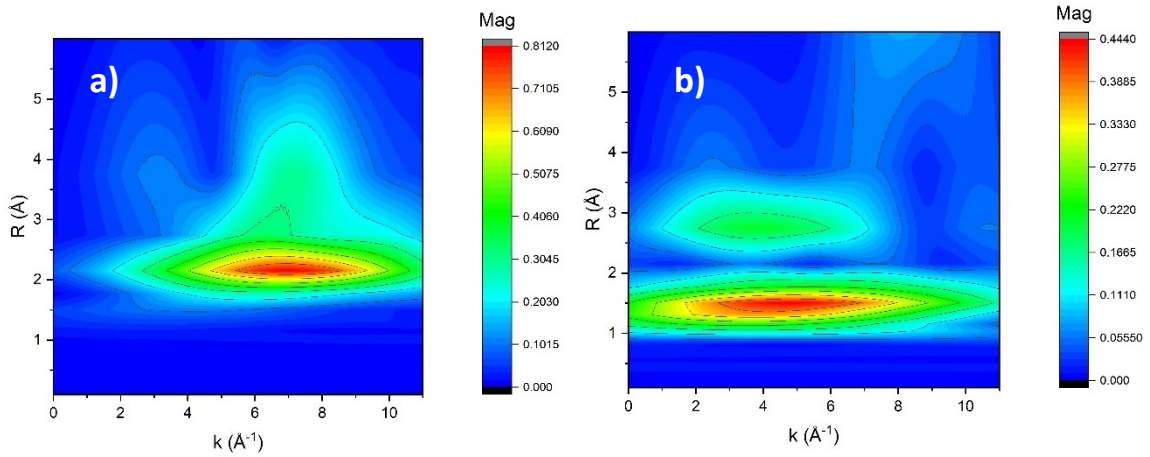

Fig. S15 Cu K edge WT contour plots of **a)** Cu foil and **b)** CuO standard.

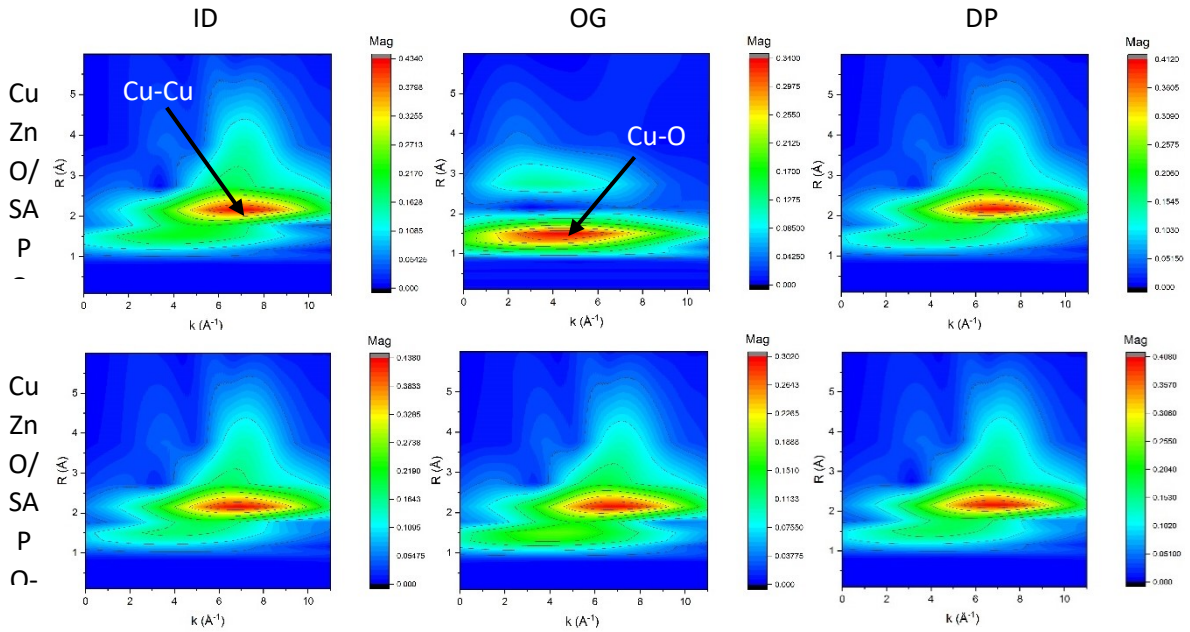

Fig. S16 Cu K edge WT contour plots of CuZnO/SAPO-11 (top) and CuZnO/SAPO-34 (bottom) catalysts prepared via the ID, OG and DP methods

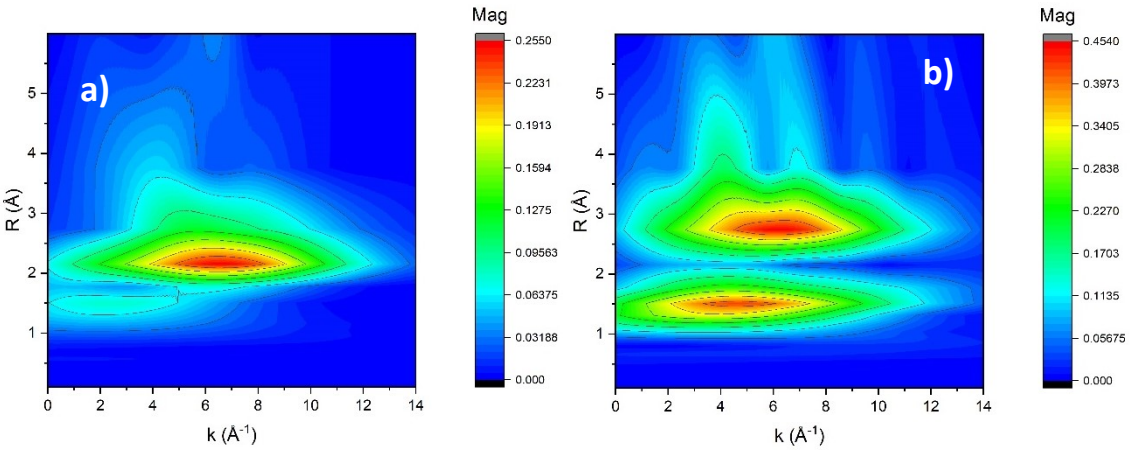

Fig. S17 Zn K edge WT contour plots of **a)** Zn foil and **b)** ZnO standard.

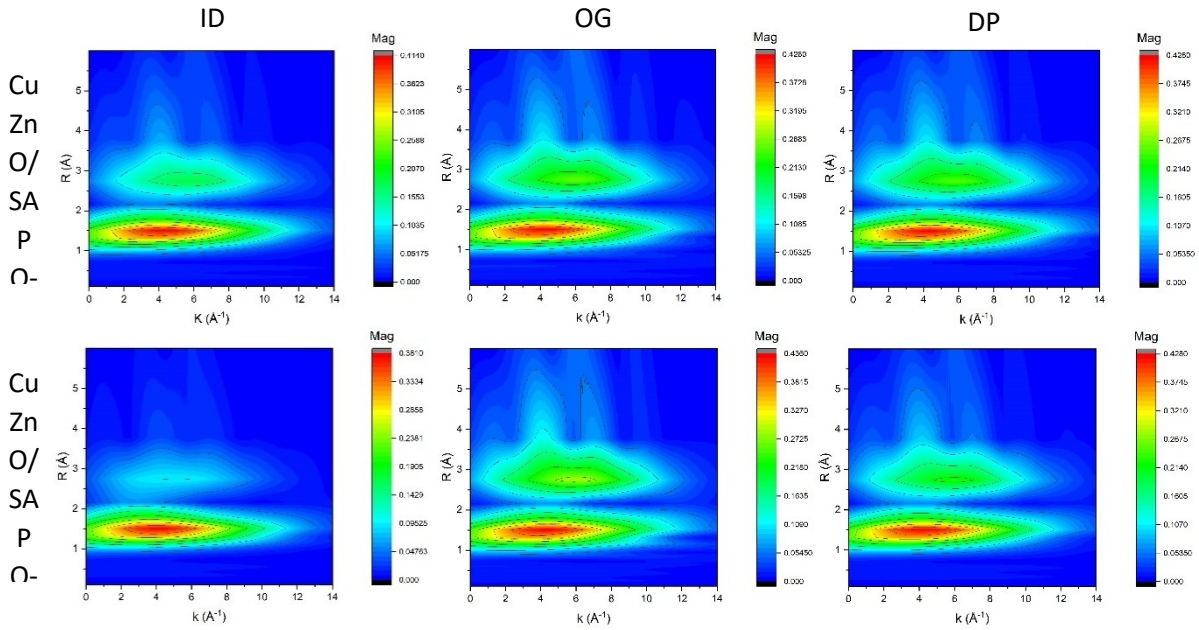

Fig. S18 Zn K edge WT contour plots of CuZnO/SAPO-11 (top) and CuZnO/SAPO-34 (bottom) catalysts prepared via the ID, OG and DP methods.

3.10 X-ray photoelectron spectroscopy (XPS)

X-ray photoelectron spectroscopy (XPS) was performed on a Thermo Fisher Scientific K-alpha$^+$ spectrometer. Samples were analysed using a micro-focused monochromatic Al x-ray source (72 W) using the "400-micron spot" mode, which provides an analysis defining elliptical x-ray spot of *ca*. 400 x 600 microns. Data was recorded at pass energies of 150 eV for survey scans and 50 eV for high resolution scans with step sizes of 1 eV and 0.1 eV respectively, the dwell time was 50 ms and 10 ms in each case. The samples were isolated from the spectrometer by mounting on to silicone free double-sided adhesive tape attached to a cut and cleaned glass microscope slide. Charge compensation was achieved using a combination of both low energy electrons and argon ions.

As Cu is known to reduce under XPS analysis, therefore, to assess the extent of reduction the Cu(2p) and Cu Auger spectra was recorded before other regions, and again at the end.

Data analysis was performed in CasaXPS v2.3.26 after calibrating the data to the lowest C(1s) component assumed to have a value of 285.0 eV.[13] Quantification was made using a Shirley type background and Scofield cross sections, with an electron energy dependence based on the TPP-2M relationship.[14] For Peak fitting, the CasaXPS LA line shape was used, and where possible spectra were modelled using fits taken from bulk species (e.g. CuO); this was especially useful in determining the at% of Al(2p) which strongly overlaps with the Cu(3p) signal.

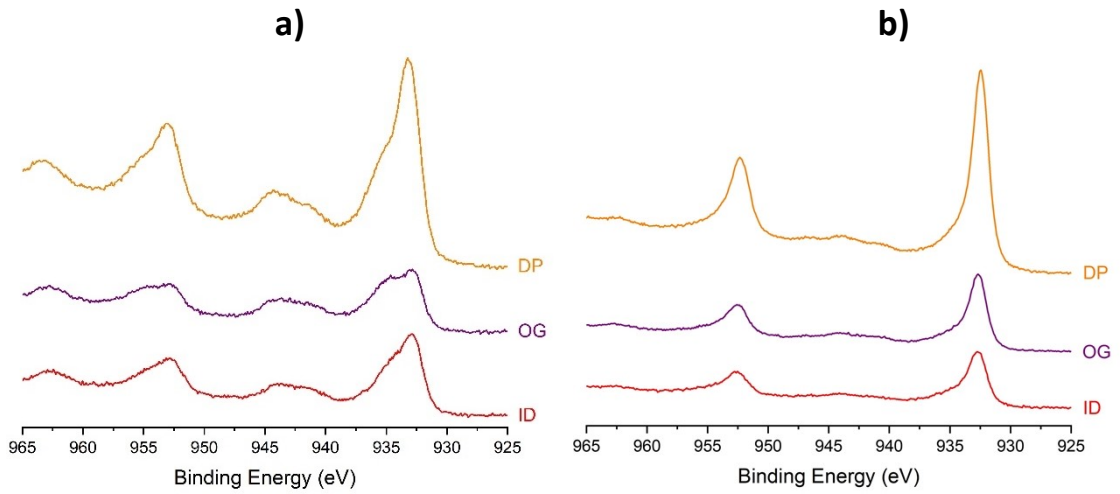

Fig. S19 Cu $2p_{3/2}$ XPS spectra of **a)** CuZnO/SAPO-11 and **b)** CuZnO/SAPO-34 catalysts prepared via various synthetic methods.

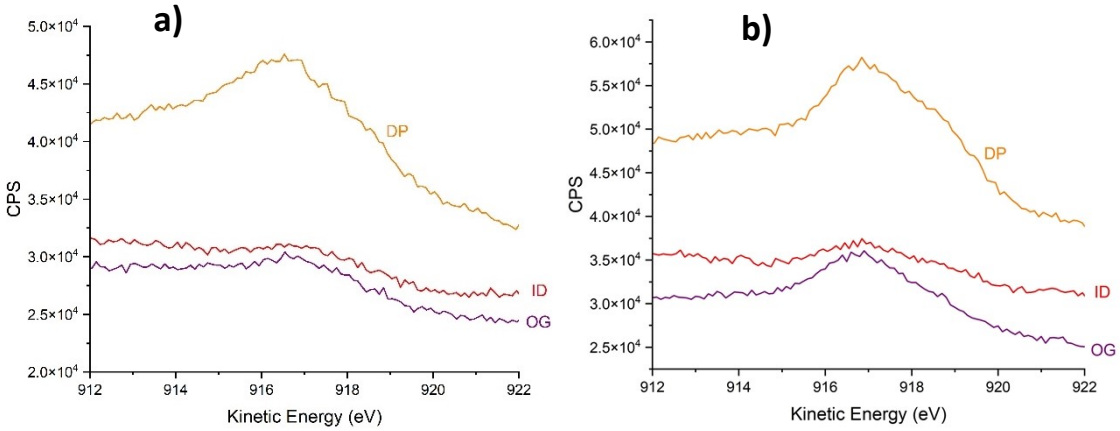

Fig. S20 Cu $L_3M_{4,5}M_{4,5}$ XPS spectra of **a)** CuZnO/SAPO-11 and **b)** CuZnO/SAPO-34 catalysts prepared via various synthetic methods.

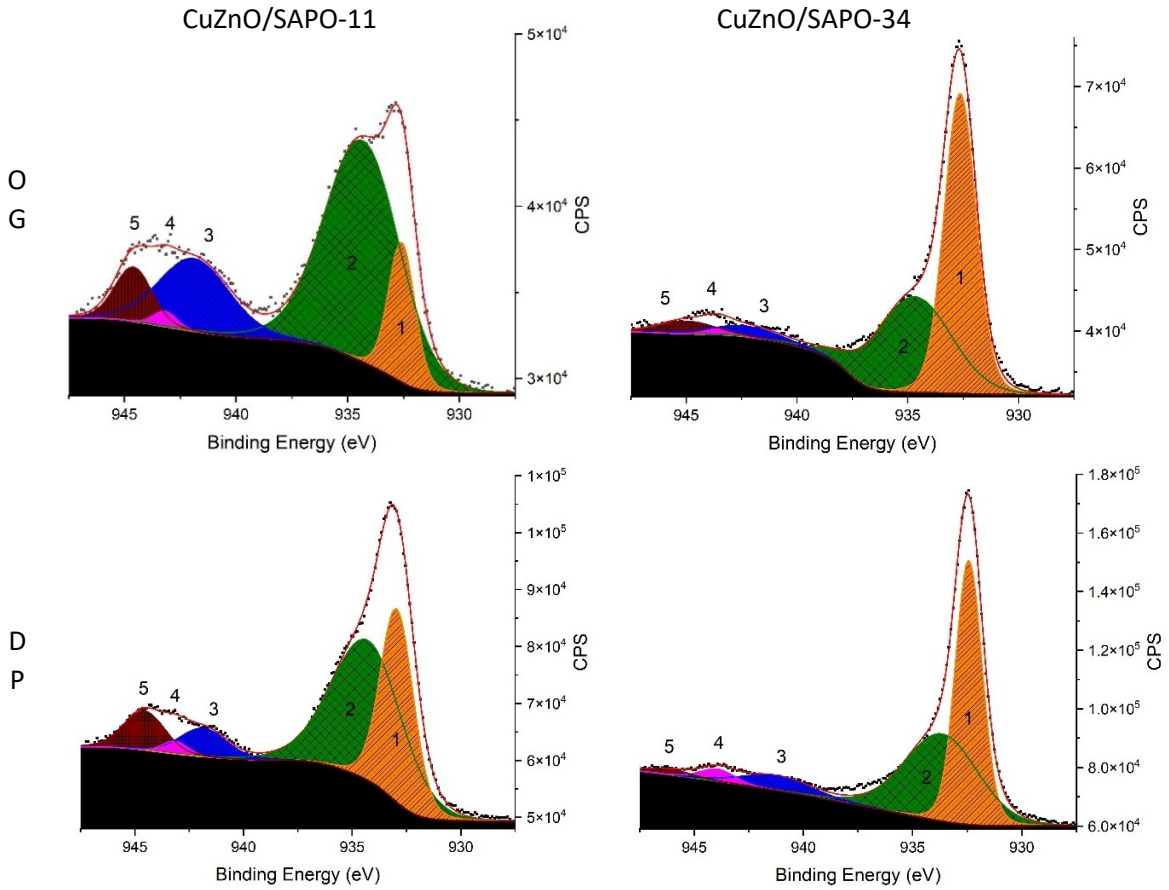

Fig. S21 Cu $L_3M_{4,5}M_{4,5}$ XPS spectra of CuZnO/SAPO-11 (left) and CuZnO/SAPO-34 (right) catalysts prepared via various synthetic methods.

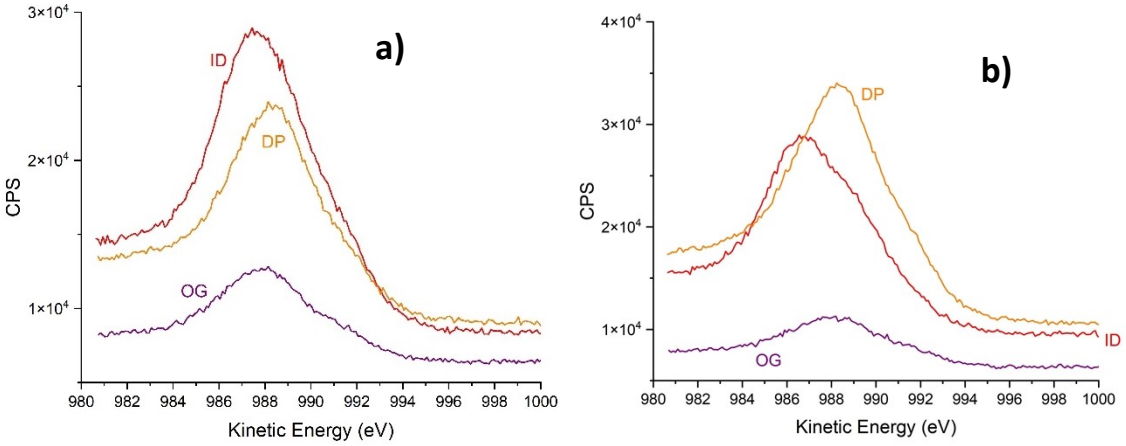

Fig. S22 Zn $L_3M_{4,5}M_{4,5}$ XPS spectra of **a)** CuZnO/SAPO-11 and **b)** CuZnO/SAPO-34 catalysts prepared via various synthetic methods.

Table S7 XPS determined Cu^{2+} and Cu^{+}/Cu^{0} content of CuZnO/SAPO-X (where X = 11 or 34) catalysts prepared via different methods

Synthesis Method	Cu^{2+} Content (%)		Cu^{+}/Cu^{0} Content (%)	
	-11	-34	-11	-34
ID	80	47	20	53
OG	87	48	13	52
DP	67	53	33	47

3.11 Characterisation overview

Table S8 Structural summary of CuZnO/SAPO-X (where X = 11 or 34) catalysts prepared via the ID, OG and DP methods.

Catalyst	NH_3-TPD Acid Site Abundance		NH_3-TPD Acid Site Strength		XRD Nanoparticle Size (nm)		XAFS Average Cu Oxidation State		Average Proximity Between Redox and Acid Sites	
	-11	-34	-11	-34	-11	-34	11	34	11	34
CuZnO/SAPO-X ID	I	H	WS	WMS	42	13	0.50	0.35	H	H
CuZnO/SAPO-X OG	I	H	W	W	8	9	1.43	0.41	I	I
CuZnO/SAPO-X DP	L	I	W	W	13	9	0.36	0.35	L	L

L stands for low, I for intermediate and H for high. W stands for weak, M stands for medium and S for strong acid strength.

4 Catalysis

4.1 Catalytic results

Table S9 Catalytic performance of M/SAPO-X (where X = 11 or 34) catalysts. Conditions: 260°C, 40 bars, 13 000 mL g^{-1} h^{-1} GHSV, 3:1 H_2:CO_2 volumetric ratio.

Catalyst	CO_2 Conversion (%)		CO Selectivity (%)		MeOH Selectivity (%)		DME Selectivity (%)		DME Yield (%)	
	-11	-34	-11	-34	-11	-34	-11	-34	-11	-34
SAPO-X ID	0	0	-	-	-	-	-	-	0	0
2:10 Cu/SAPO-X ID	<1	<1	0	0	27	34	73	66	<1	<1
1:10 Zn/SAPO-X ID	0	0	-	-	-	-	-	-	0	0
2:10 Cu/SAPO-X + 1:10 ZnO/SAPO-X PM	0	0	-	-	-	-	-	-	0	0
2:1 CuZnO ID	2		0		61		39		<1	

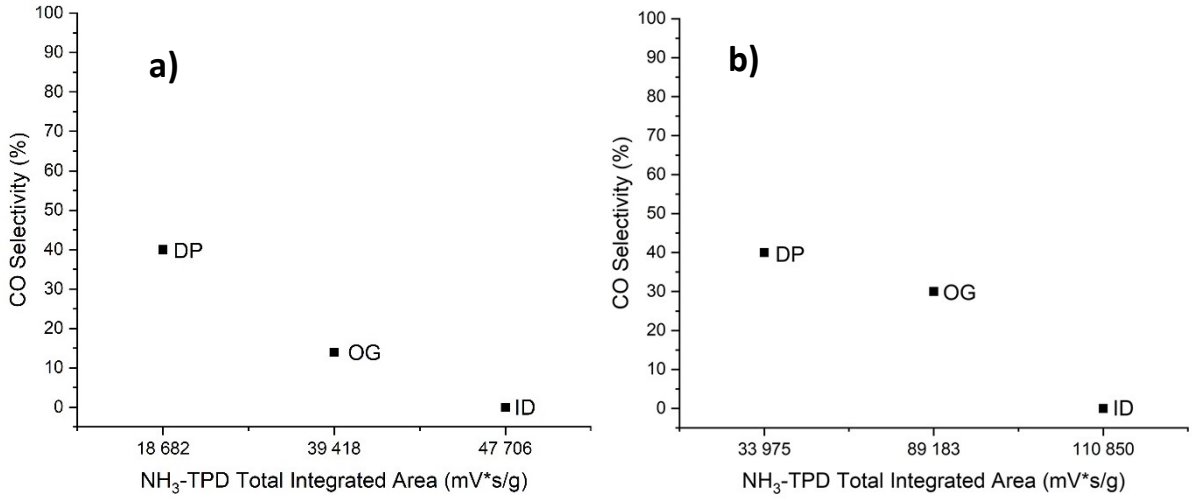

Fig. S23 Plot of total NH_3-TPD integrated area against CO selectivity for **a)** CuZnO/SAPO-11 and **b)** CuZnO/SAPO-34 catalysts produced using different methods.

Table S10 Space time yield (STY) of water for different catalysts. Conditions: 260°C, 40 bars, 13 000 mL g^{-1} h^{-1} GHSV, 3:1 H_2:CO_2 volumetric ratio.

	Water STY (g_{water} kg_{cat}^{-1} h^{-1})	
Catalyst	-11	-34
CuZnO/SAPO-X ID	33	70
CuZnO/SAPO-X OG	89	54
CuZnO/SAPO-X DP	51	33
Cu/ZnO/Al_2O_3 + SAPO-X PM	137	83
Cu/ZnO/Al_2O_3 + SAPO-X GM	99	67
Cu/ZnO/Al_2O_3 + SAPO-X DB	89	61

4.2 Time-on-stream stability

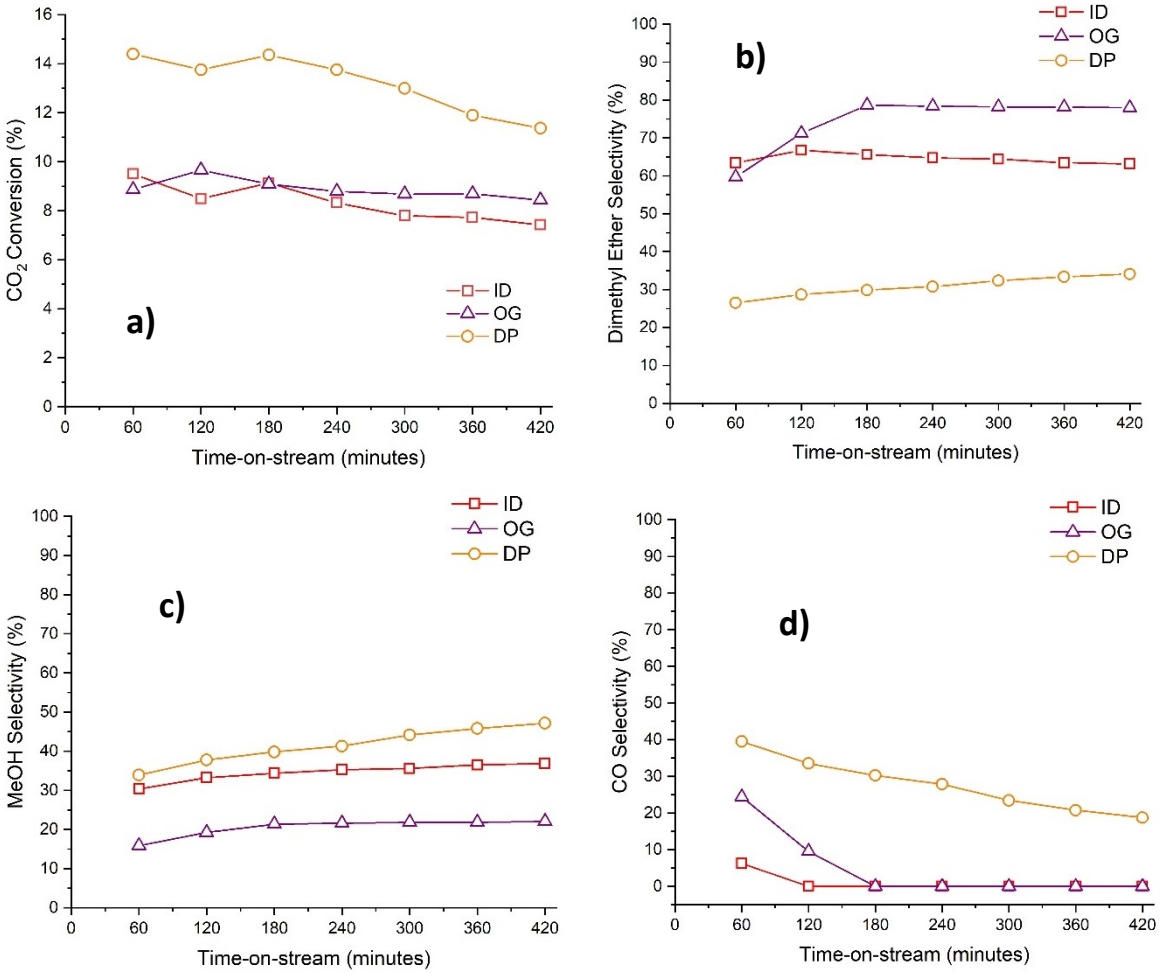

Fig. S24 Catalytic performance of CuZnO/SAPO-11 catalysts synthesised via the ID, OG and DP methods as a function of time-on-stream. **a)** CO_2 conversion **b)** DME selectivity **c)** MeOH selectivity and **d)** CO selectivity. Conditions: 260°C, 40 bars, 13 000 mL g^{-1} h^{-1} GHSV, 3:1 H_2:CO_2 volumetric ratio. Average carbon mass balance = 97%.

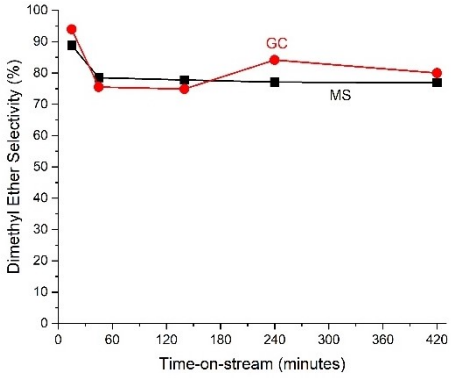

Fig. S25 Comparison of DME selectivity calculated using online mass spectrometer (MS) and offline gas chromatograph (GC) for the CuZnO/SAPO-34 ID catalyst verifying its high DME selectivity.

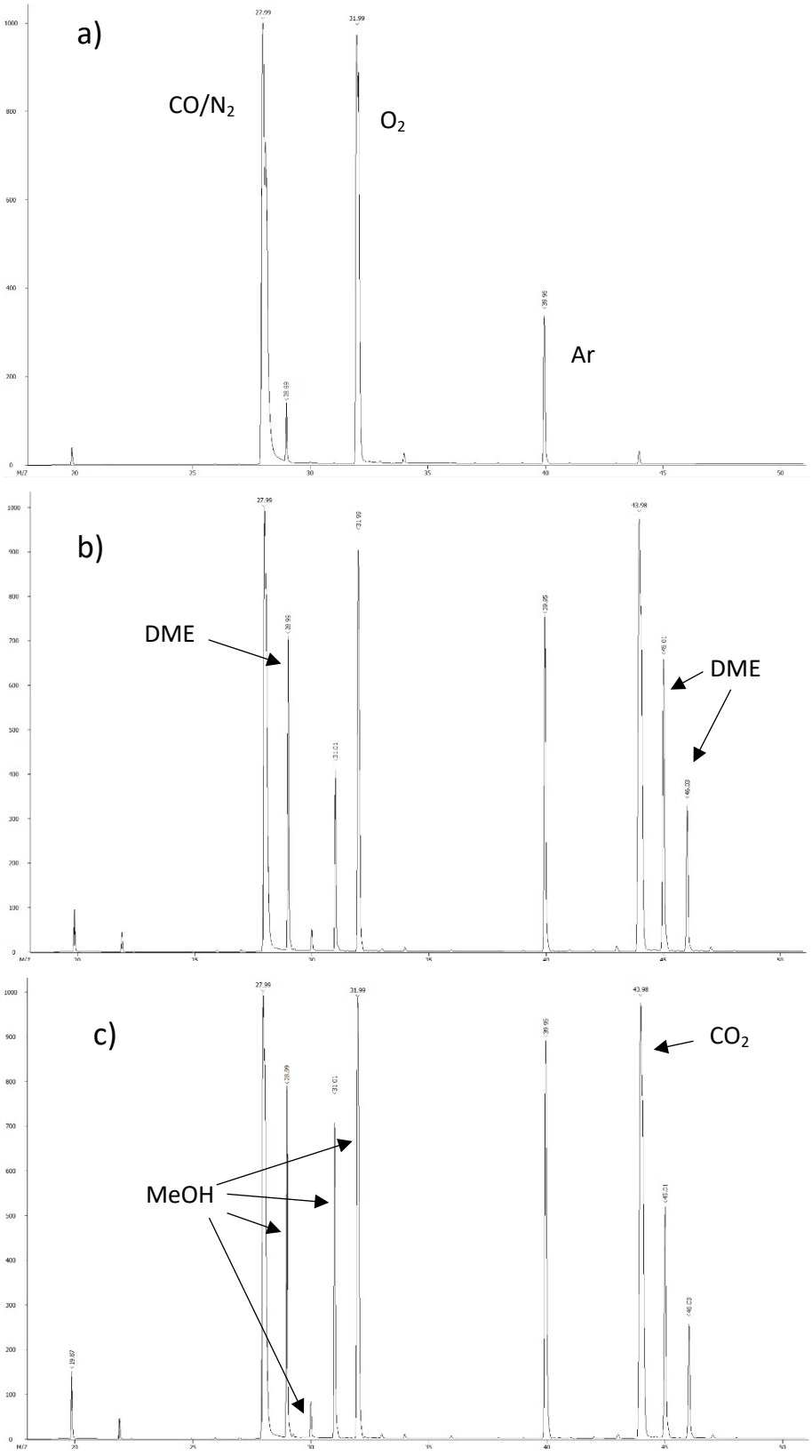

Fig. S26 Mass spectra of **a)** blank injection and exit gases at time-on-stream of **b)** 15 minutes and **c)** 420 minutes for the CuZnO/SAPO-34 ID catalyst. These results are from an uncalibrated mass spectrometer as such they are only qualitative and not quantitative.

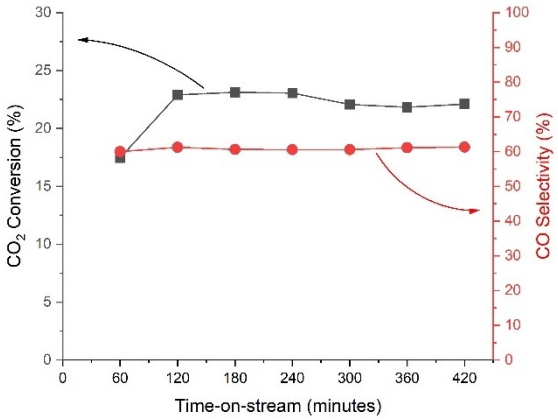

Fig. S27 Time-on-stream stability of commercial Cu-based methanol synthesis catalyst showing stable CO_2 conversion and CO selectivity during the test. Conditions: 260°C, 40 bars, 13 000 mL g^{-1} h^{-1} GHSV, 3:1 H_2:CO_2 volumetric ratio. Average carbon mass balance = 96%.

4.3 Spent catalyst characterisation

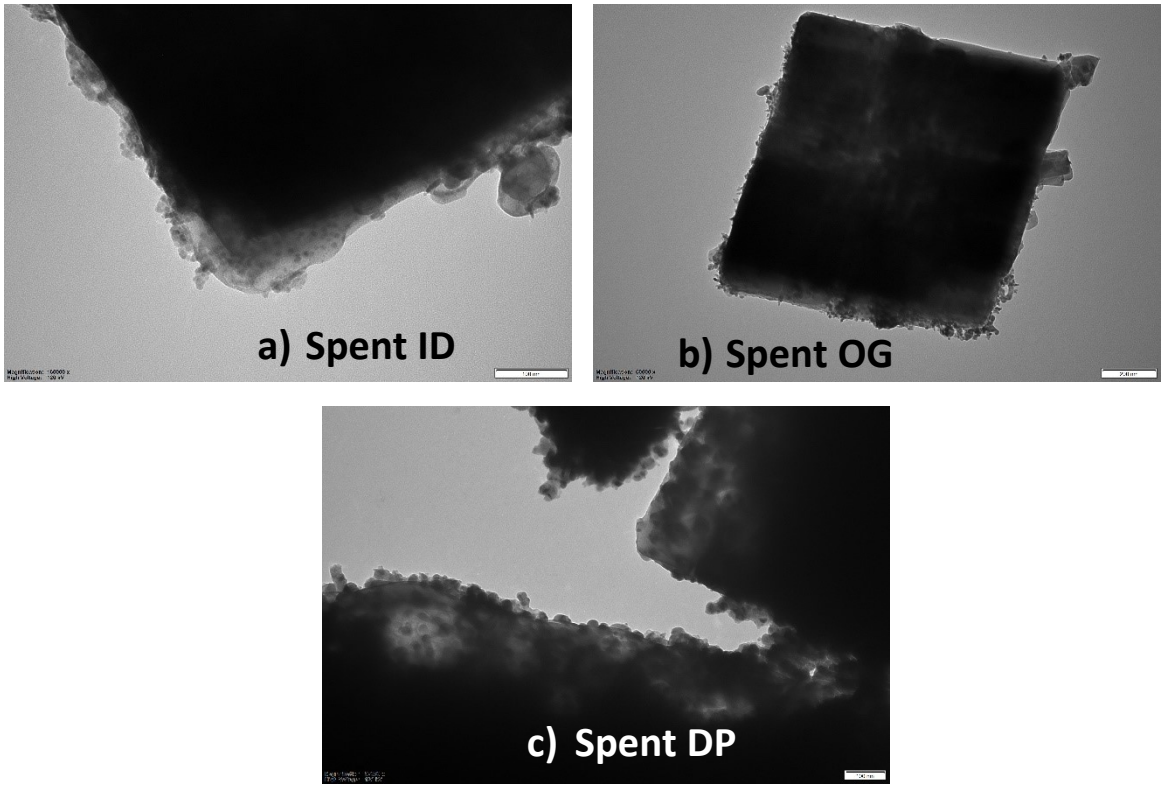

Fig. S28 TEM images of spent CuZnO/SAPO-34 catalysts prepared via ID, OG and DP methods used for time-on-stream stability testing.

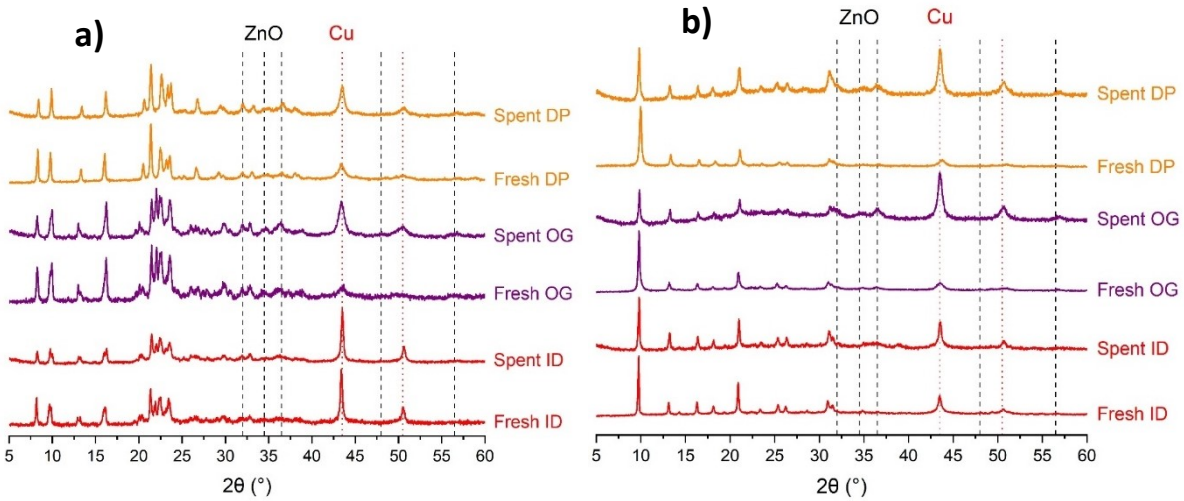

Fig. S29 PXRD patterns of spent **a)** CuZnO/SAPO-11 and **b)** CuZnO/SAPO-34 catalysts prepared via the ID, OG and DP methods compared to the fresh catalysts.

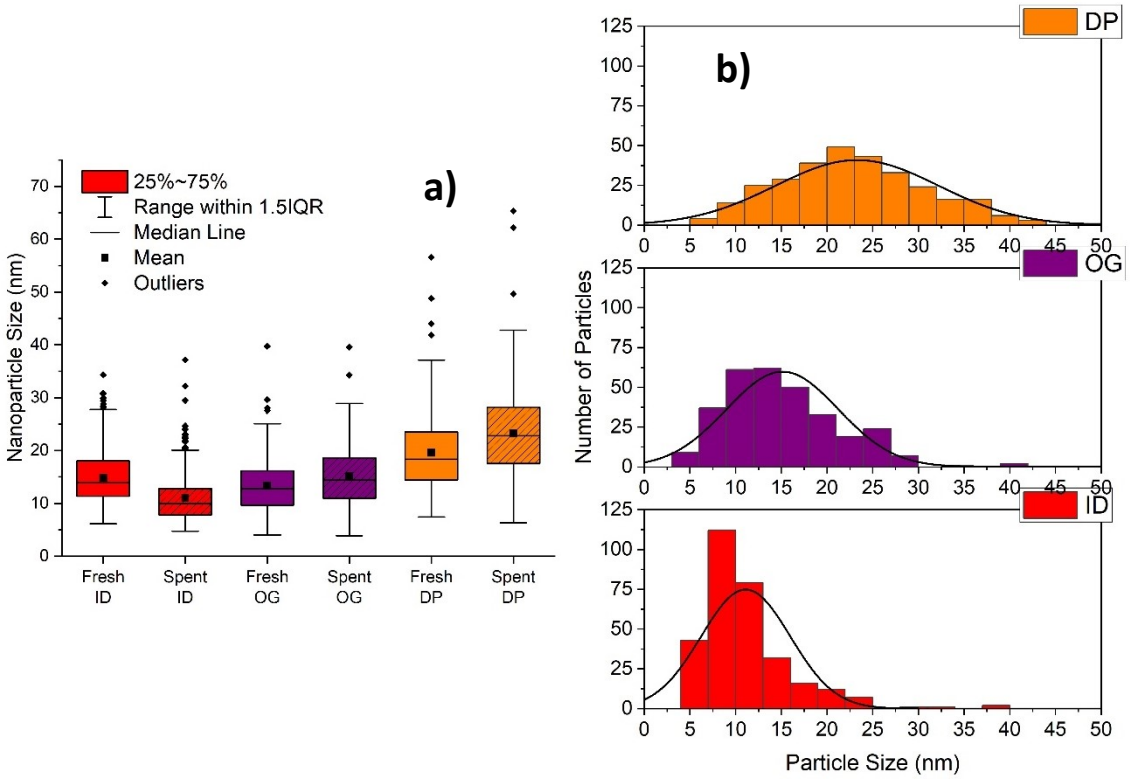

Fig. S30 a) Nanoparticle size distribution of fresh vs spent CuZnO/SAPO-34 catalysts prepared via ID, OG and DP methods. **b)** Particle size histograms of spent CuZnO/SAPO-34 catalysts prepared via ID, OG and DP methods. All results based on a measurement of 300 nanoparticles

Table S11 Total surface area of fresh powder, fresh pelletised and spent pelletised CuZnO/SAPO-X (where X = 11 or 34) catalysts prepared via the ID, OG and DP methods.

	Fresh Powder (m^2/g)		Fresh Pelletised (m^2/g)		Spent Pelletised (m^2/g)	
Catalyst	-11	-34	-11	-34	-11	-34
ID	21	330	8	228	11	246
OG	92	245	36	115	30	125
DP	30	274	12	191	8	194

4.4 Catalyst comparison

Table S12 Comparison of physiochemical characteristics of various catalysts used for one-pot conversion of CO_2 to DME.

Catalyst	Cu Loading (wt%)	Nanoparticle Size (nm)	Acid Strength	Acid Site Quantity	Redox-Acid Site Proximity	BET Surface Area (m^2/g)	Ref.
CuZnO/SAPO-34 ID	**13**	**15**	**WMS**	**H**	**H**	**330**	**This Work**
Cu-In-Zr-O + SAPO-34	17.93	30.1	-	-	I	-	[9]
CuZnO/ZSM-5 CVI	9.7	76	MS	M	H	297	[15]
CuZnO/ZSM-5 OG	9.7	15	MS	M	I	303	[15]
PdZn/ZSM-5	-	5.5	M	M	H	334.7	[8]
Cu-ZnO-ZrO_2 +ZSM-5	-	-	WMS	H	L	-	[16]
Cu-ZnO-ZrO_2/FER	-	8	WM	M	I	182	[17]
Cu-ZnO-ZrO_2/MOR	-	8	WS	L	I	217	[17]
Cu-ZnO-ZrO_2-Al_2O_3/ZSM-5	-	7.7	WMS	H	L	-	[18]

Table S13 Comparison of catalytic performance of various catalysts used for one-pot conversion of CO_2 to DME.

Catalyst	Preparation Method	T (°C)	P (bar)	GHSV (h^{-1})	*X* CO_2 (%)	*S* DME (%)	*S* MeOH (%)	*S* CO (%)	Ref.
CuZnO/SAPO-34 ID	**ID**	**260**	**40**	**13,000**	**8**	**80**	**20**	**0**	**This Work**
Cu-In-Zr-O + SAPO-34	PM	250	30	6000	~4.4	~60	~32	~8	[9]
CuZnO/ZSM-5	CVI	250	20	3600	3.4	22.1	6.4	71.5	[15]
CuZnO/ZSM-5	OG	250	20	3600	13.8	27.5	4.0	68.4	[15]
PdZn/ZSM-5	CVI	270	20	3500	14	30.4	4.2	65.3	[8]
Cu-ZnO-ZrO_2 +ZSM-5	PM	240	30	10,000	16.1	33.9	11.8	54.3	[16]
Cu-ZnO-ZrO_2/FER	OG	280	50	8800	~29	~62	~14	~24	[17]
Cu-ZnO-ZrO_2/MOR	OG	280	50	8800	~26	~51	~11	~38	[17]
Cu-ZnO-ZrO_2-Al_2O_3/ZSM-5	PM	240	28	917	26.5	69.2	~8	~23	[18]

References

1 K. V. V. S. B. S. R. Murthy, S. J. Kulkarni and S. K. Masthan, *Microporous and Mesoporous Materials*, 2001, **43**, 201–209.

2 M. E. Potter, L. M. Armstrong and R. Raja, *Catal. Sci. Technol.*, 2018, **8**, 6163–6172.

3 Q. Sun, Y. L. Zhang, H. Y. Chen, J. F. Deng, D. Wu and S. Y. Chen, *J. Catal.*, 1997, **167**, 92–105.

4 C. Baltes, S. Vukojević and F. Schüth, *J. Catal.*, 2008, **258**, 334–344.

5 S. Wang, P. Wang, D. Shi, S. He, L. Zhang, W. Yan, Z. Qin, J. Li, M. Dong, J. Wang, U. Olsbye and W. Fan, *ACS Catal.*, 2020, **10**, 2046–2059.

6 M. Sánchez-Contador, A. Ateka, A. T. Aguayo and J. Bilbao, *Fuel Processing Technology*, 2018, **179**, 258–268.

7 A. Ateka, A. Portillo, M. Sánchez-Contador, J. Bilbao and A. T. Aguayo, *Renew. Energy*, 2021, **169**, 1242–1251.

8 H. Bahruji, R. D. Armstrong, J. Ruiz Esquius, W. Jones, M. Bowker and G. J. Hutchings, *Ind. Eng. Chem. Res.*, 2018, **57**, 6821–6829.

9 L. Yao, X. Shen, Y. Pan and Z. Peng, *Energy and Fuels*, 2020, **34**, 8635–8643.

10 B. Ravel and M. Newville, *J. Synchrotron Radiat.*, 2005, **12**, 537–541.

11 H. Funke, A. C. Scheinost and M. Chukalina, *Phys. Rev. B*, 2005, **71**, 094110.

12 (PDF) A Program for Wavelet Transform of EXAFS Data from Athena, https://www.researchgate.net/publication/338644183_A_Program_for_Wavelet_Transform_of_EXAFS_Data_from_Athena?channel=doi&linkId=6031c21b299bf1cc26dda245&showFulltext=true, (accessed 27 February 2024).

13 N. Fairley, V. Fernandez, M. Richard-Plouet, C. Guillot-Deudon, J. Walton, E. Smith, D. Flahaut, M. Greiner, M. Biesinger, S. Tougaard, D. Morgan and J. Baltrusaitis, *Applied Surface Science Advances*, 2021, **5**, 100112.

14 S. Tanuma, C. J. Powell and D. R. Penn, *Surface and Interface Analysis*, 2003, **35**, 268–275.

15 A. Tariq, J. Ruiz Esquius, T. E. Davies, M. Bowker, S. H. Taylor and G. J. Hutchings, *Top. Catal.*, 2021, **64**, 965–973.

16 G. Bonura, M. Cordaro, L. Spadaro, C. Cannilla, F. Arena and F. Frusteri, *Appl. Catal. B*, 2013, **140–141**, 16–24.

17 G. Bonura, F. Frusteri, C. Cannilla, G. Drago Ferrante, A. Aloise, E. Catizzone, M. Migliori and G. Giordano, *Catal. Today*, 2016, **277**, 48–54.

18 S. Ren, X. Fan, Z. Shang, W. R. Shoemaker, L. Ma, T. Wu, S. Li, N. B. Klinghoffer, M. Yu and X. Liang, *Journal of CO2 Utilization*, 2020, **36**, 82–95.